

## ACOUSTIC DETECTION AND TRACKING OF A PIPELINE INSPECTION GAUGE

Giancarlo Bernasconi (\*), Politecnico di Milano, Milan

Giuseppe Giunta, Eni S.p.A, Development Operations & Technology, San Donato Milanese

\* *Corresponding author: G. Bernasconi (giancarlo.bernasconi@polimi.it)*

### ABSTRACT

Pipeline Inspection Gauges (PIGs) are widely used for monitoring and managing pipeline integrity. During a pigging operation it is fundamental to have a continuous measurement of the PIG position and movement, in order to achieve the best inspection and to have an early warning in the case the device is stuck. Currently, the tracking is performed by installing on the PIG “active” systems (e.g. acoustic pingers or electromagnetic emitters) that communicate with a set of receivers, making it possible the localization of the travelling gauge. Another solution is the deployment of an appropriately dense network of sensors along the pipe track, or the utilization of a dedicated system/crew that moves close to the pipe, so to physically perceive the vibrations generated by the nearby passage of the device. In fact, the moving PIG produces pressure transients and vibro-acoustic noise due to the velocity fluctuations, to the friction against the internal walls and to the crossing of the welding dents. It is important to mention that the conduit acts like an acoustic waveguide and the “sound” generated by the PIG, in many practical situations, can be sensed within the fluid at several kilometres from the originating point. This paper presents three different tracking procedures that exploit the noise generated by the PIG to locate it, remotely and passively, without requiring any additional equipment to be mounted on the gauge. The key points of the procedures are the availability of pressure measurements at a small number of positions along the pipeline, at relative distances of tens of kilometres, an accurate synchronization of the measurements, the real time transmission and multichannel processing of the data. The first method locates the PIG by performing a crosscorrelation analysis between the acoustic signal recorded on opposite sides of the moving gauge, the second method is based on the counting of the transients generated at known positions, the third one describes the pipe section between the PIG and the arrival terminal like a resonant structure, and obtains the length of this section (the distance of the PIG to the arrival) from the resonance frequency. All the methods are presented starting from real examples, in order to highlight their effective applicability. Moreover, the localization results are in agreement with the output of more sophisticated technological solutions.

**Keywords:** pipeline inspection; PIG tracking; pressure transients

### 1. INTRODUCTION

Pipeline Inspection Gauges (PIGs) are used to perform various integrity operations in fluid transportation pipelines. PIGs are usually inserted in the conduit in a “launcher” station, and then they are pushed by the flow itself up to a “receiving” trap (Tiratsoo, 1999).

Some of these devices are used to remove deposits inside the pipeline, others contain measuring instrumentation able to inspect the condition of the pipe walls (InLine Inspection tools: ILI), and others collect objects and/or dust that have been dispersed along the track (Hiltscher et al, 2003). In all cases it is extremely important to know the position of the PIG and to recognise whether it has

possibly got stuck. Moreover, some ILI tools, like the Magnetic Flux Leakage (MFL) and the UltraSonic (US) devices, are effective in a limited range of displacement velocity, so that a real time tracking can permit the utilization of active PIG velocity control procedures (Liang et al., 2017; Chen et al, 2018).

Nowadays there exist various systems for locating and/or tracking a PIG inside a generic pipeline (McAllister, 2009). For example, the conventional method estimates the PIG position by measuring the pressure and the volume of fluids entering and exiting the line, upstream and downstream of the device (Nguyen et al., 2001). The more efficient implementations of this approach execute an optimization loop using dynamic flow simulators and get the position and velocity of the gauge, treated as a moving singular boundary, by fitting the measured fluid inventory with the output of the simulator (Patricio et al, 2020), also in multiphase scenarios (Tolmasquim et al., 2008; Davoudi et al., 2014).

Other systems perform a direct “on the field” identification of the vibrations produced by the PIG during its movement. In fact, when the sealing cups of the PIG encounter a weld or a variation of the inner section, vibrational and acoustic signals are generated (Hendrix et al., 2018). These vibrations can be sensed by a network of geophones (Brown et al, 1986) or by an optical fibre acting like a Distributed Acoustic Sensing (DAS) device (Barrias et al., 2016; Hartog, 2017; Tanimola et al., 2009). In offshore scenarios it is possible to make use of submarine ROVs to follow and to validate the gauge passage (McAllister, 2009).

An alternative solution is to mount active sources on the PIG, e.g. electromagnetic (Brayson, 1997) or acoustic emitters (Alonso, 2009), and to deploy along the pipe track a network of corresponding receivers.

Finally, there are also methods to locate a PIG that is stuck in a pipeline: one technique is based on the generation of suitable hydraulic transients within the fluid on the pipe branch where the PIG is blocked, measuring then the return times of the echoes that are generated on the device (Gudmundsson, 2017). In all cases the range of detection depends on the pipeline diameter, on the filling fluid and on the type of PIG, from few kilometres up to tens of kilometres.

Smart PIGs have a gyroscopic self-location unit, in order to tag the position of the measured anomalies (Wang et al., 2010; Chowdhury et al., 2016). Self-positioning data is not available in real time, but it is downloaded only when the pigging run has been completed, and it has to be checked with external logs for verification and calibration. Please note that the PIG itself cannot receive GPS signal when travelling within a metal pipe.

Therefore, a first group of systems that locate and/or follow a PIG inside a pipeline measure and process the signals collected by a plurality of sensors arranged along the pipeline itself. Such solutions have a series of drawbacks. A first drawback is the number of measuring points needed to obtain a good accuracy in locating the PIG. It can moreover be costly and complicated to provide such stations, particularly in deep offshore or underground pipes. Moreover, the methods that rely on passive measurements, like for example the vibrations generated by the PIG movement, do not work when the device is blocked inside the pipe, or at least give the position of the last triggered receiver. Another group of location systems need an active source on board of the PIG: in other words, special devices must be used, with a consequent increase in the costs and in the constructive complexity.

This paper presents three different procedures for a continuous PIG localization/tracking that exploit the passive vibroacoustic signals generated by the travelling gauge, recorded by stations located at tens of kilometres between each other along the conduit. The key points of the procedures are the accurate synchronization of the measuring units, the use of high sensitivity

sensors, the accurate selection of the useful bandwidth, the real time transmission and multichannel processing of the data (Giunta et al., 2017a and 2017b).

The first method is based on a crosscorrelation analysis for the extraction of the differential time of arrival of the acoustic signals generated by the PIG and recorded at opposite sides of it (Carter, 1985).

The second method is based on the counting of the acoustic wavelets generated by the PIG when crossing the welding dents, and on their mapping according to the pipeline construction book.

The third method works when the PIG moves in a “start and stop” fashion: the line section limited by the PIG behaves like a resonant structure, where the resonant frequency is a function of the section length, i.e. of the PIG position.

All these methods are able to obtain continuously and in real time the position of the PIG, and so to compute its velocity as well as to identify a stuck condition. The following sections present the tracking procedures, starting from real data examples. The last section describes a mathematical model of acoustic wave propagation in pipelines, used to validate the experimental results and to compute the maximum PIG tracking distance.

## 2. OFFSHORE SCENARIO: MESSINA CHANNEL GAS PIPELINES

Several subsea pipelines cross the Messina channel transporting natural gas from North Africa to Messina (Sicily) and then to continental Italy. The lines are managed by SNAM RETE GAS. An experimental campaign of vibroacoustic monitoring has been performed on two of those lines, specified and shown in Figure 1 (Bernasconi et al., 2013, 2014).



Figure 1. Messina channel subsea natural gas transportation pipelines. In red the tracks of LINE 1 (15.9 km length, internal diameter ID=20") and LINE 4 (31.3 km length, internal diameter ID=26").

During the recording interval, some PIGs have been used in LINE1 (May 2013) and in LINE4 (October 2013), as summarized in Table 1.

PIG #	Line #	Date	PIG type
PIG1	LINE1	May 7 <sup>th</sup> 2013	cleaning
PIG2	LINE1	May 9 <sup>th</sup> 2013	ILI - MFL
PIG3	LINE1	May 28 <sup>th</sup> 2013	ILI - MFL
PIG4	LINE4	October 24 <sup>th</sup> 2013	ILI - MFL

Table 1. PIG operations on the Messina channel pipelines.

A proprietary vibroacoustic monitoring technology (e-*vpms*<sup>®</sup>) (Giunta et al., 2017c) has recorded the absolute pressure and the pressure transients within the flowing gas at the starting (Messina) and ending terminals (Favazzina and Palmi): no instrumentation is used in the offshore portion of the pipeline. Figure 2 shows the standard deviation of dynamic pressures at Messina and Favazzina, during the pigging operation PIG1 (Table 1). The plotted values are computed every 10s on the full bandwidth signal (0-1000Hz). The inspection operation, from 6:20 to 8:07 (GMT+0 time), produces a sound level above the “environmental” noise, i.e. the sound level before or after the inspection. Figure 3 is a zoom of the pressure variations: it reveals the pressure peaks generated by the sealing discs of the PIG passing through the welding dents, 12 m apart one from the other: sound maxima amplitudes are around 2-5kPa (20-50mbar), depending on the distance from the recording station.

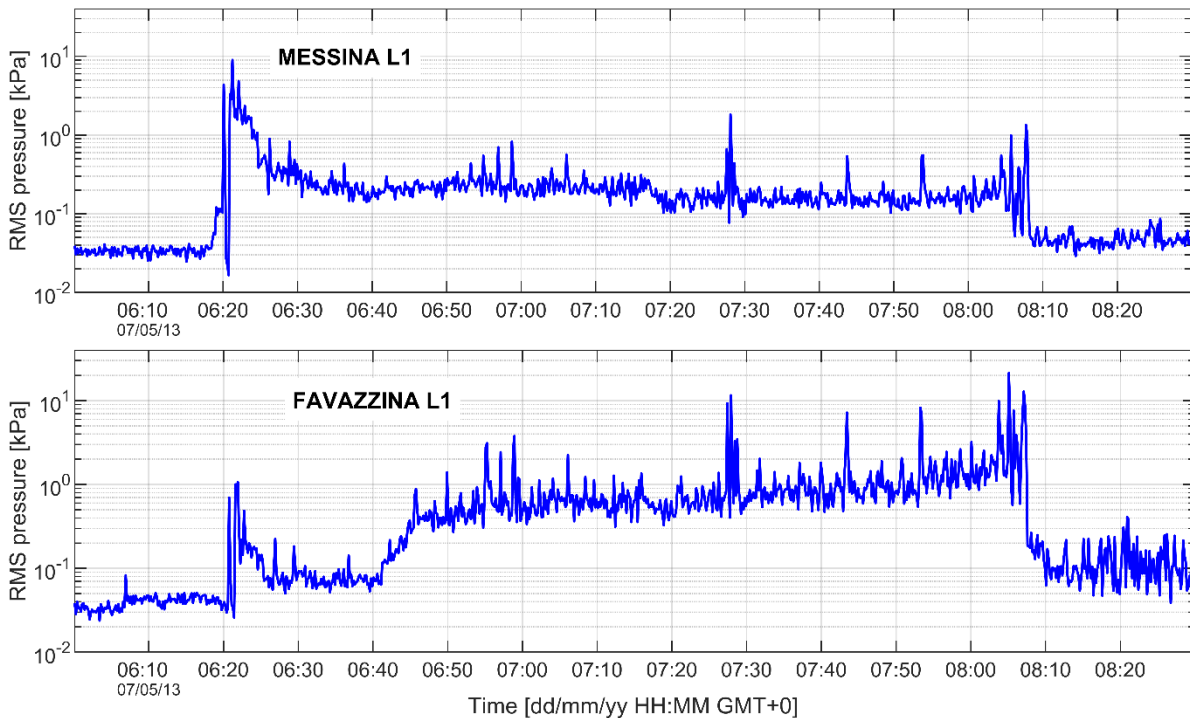


Figure 2. Dynamic pressure standard deviation computed every 10 s for PIG1 at Messina terminal (L1) and at Favazzina terminal (L1) (GMT+0 time).

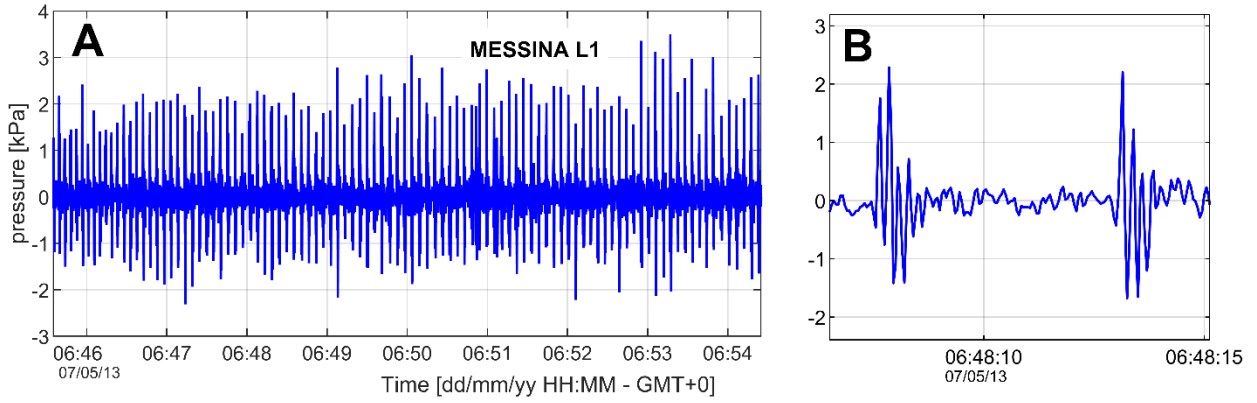


Figure 3. Dynamic pressure at Messina terminal for PIG1 in LINE1: zoom on 8 minutes in (A), zoom on 20 s in (B). Time axis in GMT+0.

2.1. PIG tracking method 1: crosscorrelation data analysis

When the sealing disc of the PIG arrives at a girth weld, there is a “climbing stage” that produces a deceleration of the gauge. Then the disc reaches the exit slope of the weld, and the gauge accelerates again (Zhang et al., 2015). The deceleration and acceleration process generates a pressure transient of opposite signs on the two sides of the PIG, that propagates at the sound speed up to the vibroacoustic monitoring stations.

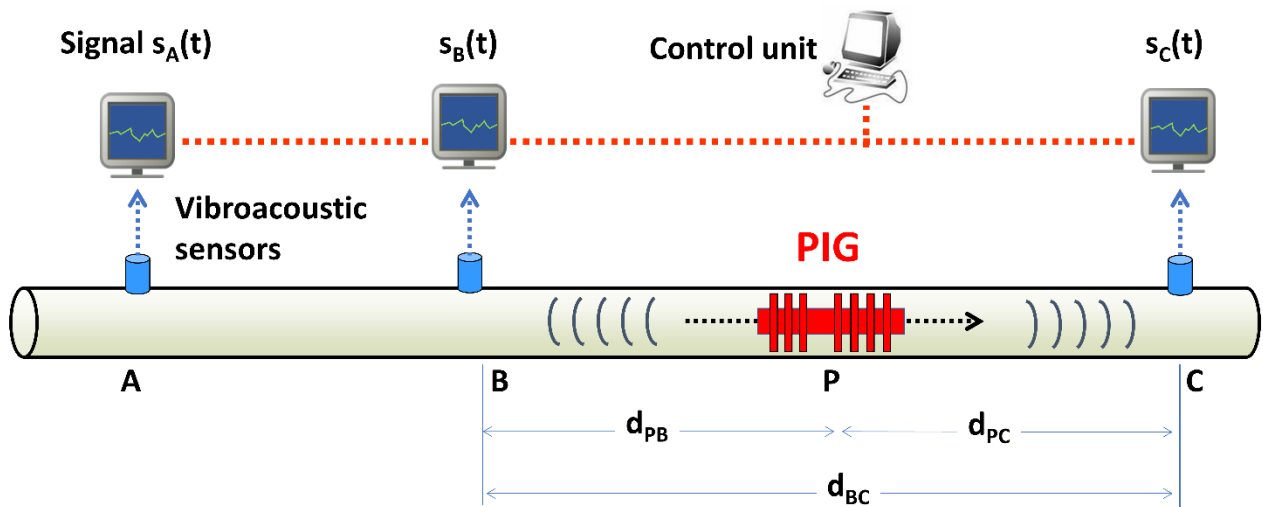


Figure 4. Moving PIG and vibroacoustic monitoring system scheme.

Referring to Figure 4 and considering the nearest recording stations on the two sides of the PIG (station B on the departing side, C on the arrival one), the acoustic “signature” generated at the weld dent in position P is recorded in  $s_B(t)$  and in  $s_C(t)$  after a propagation time  $\tau_{PB}$  and  $\tau_{PC}$ , respectively:

$$\tau_{PB} = \frac{d_{PB}}{v_{sound}}, \tag{1}$$

$$\tau_{PC} = \frac{d_{PC}}{v_{sound}},$$

$$\tau_{BC} = \tau_{PB} + \tau_{PC} = \frac{d_{BC}}{v_{sound}},$$

where  $v_{sound}$  is the sound speed in the fluid.

The crosscorrelation between  $s_B(t)$  and  $s_C(t)$  can be used to detect similarities (corresponding to a peak in the absolute value of the crosscorrelation) and the relative position (time delay of the peak value) of the similar trend (Carter, 1985). In practice the two signals are analyzed in moving windows, looking for a peak in the absolute value of the complex envelope of the normalized crosscorrelation

$$x(\tau) = \left| \text{HT} \left[ \frac{\int_{-T/2}^{T/2} s_B(t) s_C(t+\tau) dt}{\sqrt{\int_{-T/2}^{T/2} s_B^2(t) dt} \cdot \sqrt{\int_{-T/2}^{T/2} s_C^2(t) dt}} \right] \right|, \quad (2)$$

where HT is the Hilbert transform and T is the duration of the window (Feldman, 2009).

The temporal position of the peak, corresponds to the differential propagation time between the source position (PIG) and the recording stations

$$\tau_{peak} = \tau_{PB} - \tau_{PC}. \quad (3)$$

In fact, as the PIG travels through the pipe, the differential delay moves from negative (first arrival at departing station,  $\tau_{PB} < \tau_{PC}$ ), to zero (equal propagation time, the PIG is in the middle of the pipeline section,  $\tau_{PB} = \tau_{PC}$ ), and then to positive (first arrival at arrival station,  $\tau_{PB} > \tau_{PC}$ ). Rearranging equations (1) and (3), the time of the crosscorrelation peak gives the position of the PIG with respect to the measuring stations

$$d_{PB} = \frac{d_{BC} + \tau_{peak} \cdot v_{sound}}{2}; \quad (4)$$

$$d_{PC} = d_{BC} - d_{PB}.$$

The sound speed in the fluid is computed experimentally by tracking some important pressure variation along the line, possibly before the pigging campaign. In this way the correlation time axis is converted to distance along the line, and the crosscorrelation results of successive windows are presented as a 2D “waterfall” image that permits a visual awareness of the traveling PIG.

Figure 5 left is the result for PIG1 (Table 1), when correlating the acoustic signal at Messina with the acoustic signal at Favazzina. The PIG departs from Messina terminal at around 6:20 (GMT+0) and arrives in Favazzina terminal at around 8:07 (GMT+0). The sound velocity in gas can be estimated by observing the peak delay at the departure time, equal to 40 s:

$$v_{sound} = 15900\text{m}/40\text{s} = 397.5 \text{ m/s}. \quad (5)$$

Crosscorrelation moving windows are 2 minutes long, overlapped by 20 s. The white arrow in Figure 5 left indicates a change of slope in the PIG position versus recording time: it corresponds to a device velocity reduction from 4 m/s to 2.5 m/s.

Figure 5 right is the result for PIG2 (Table 1). Here it is interesting to identify two PIG stops: velocity goes to zero and the correlation peaks disappears (white arrows).

Figure 6 and Figure 7 refer to another PIG traveling from Messina to Favazzina, on May 28th, 2013 (PIG3, Table 1). Figure 6 compares the positive envelope of  $x(t)$  with the raw crosscorrelation (Feldman, 2009). As mentioned in the previous section, the moving PIG, for a positive acceleration, produces a compression of the fluid column on the advancing side and a decompression on the opposite side.

PIG on board position recordings are available, and they are compared with the results achieved by tracking the peaks along the crosscorrelation waterfall. In Figure 7 “vmin” (red line) and “vmax” (blue line) are, respectively, the minimum and maximum velocity of the gauge as measured by the on-board system, the black line is the result of the crosscorrelation procedure: the agreement is very good.

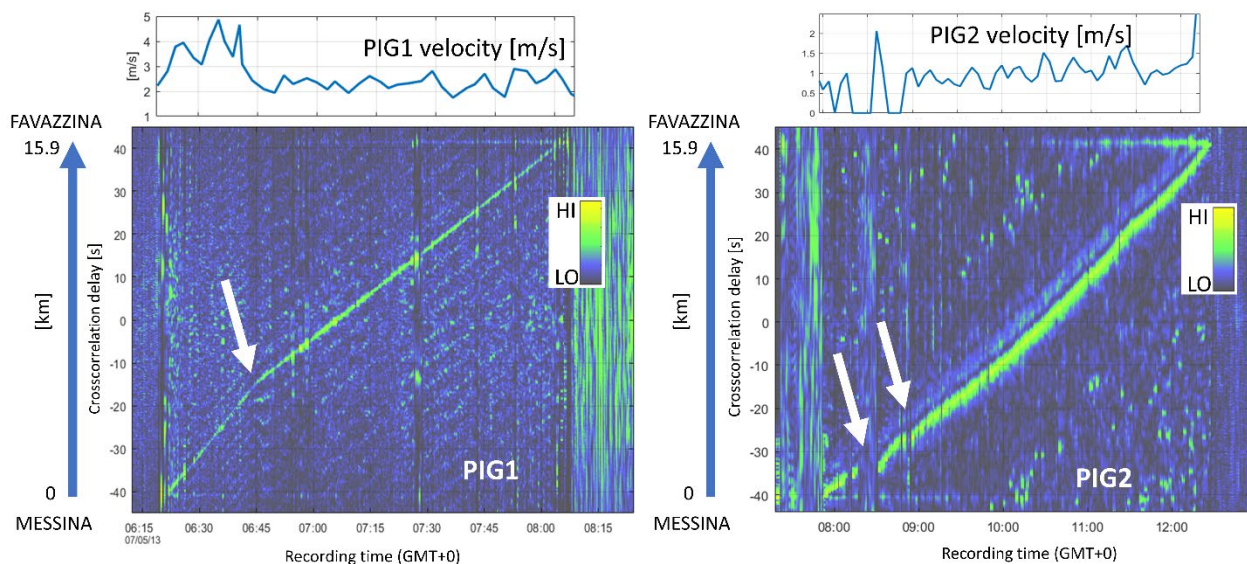
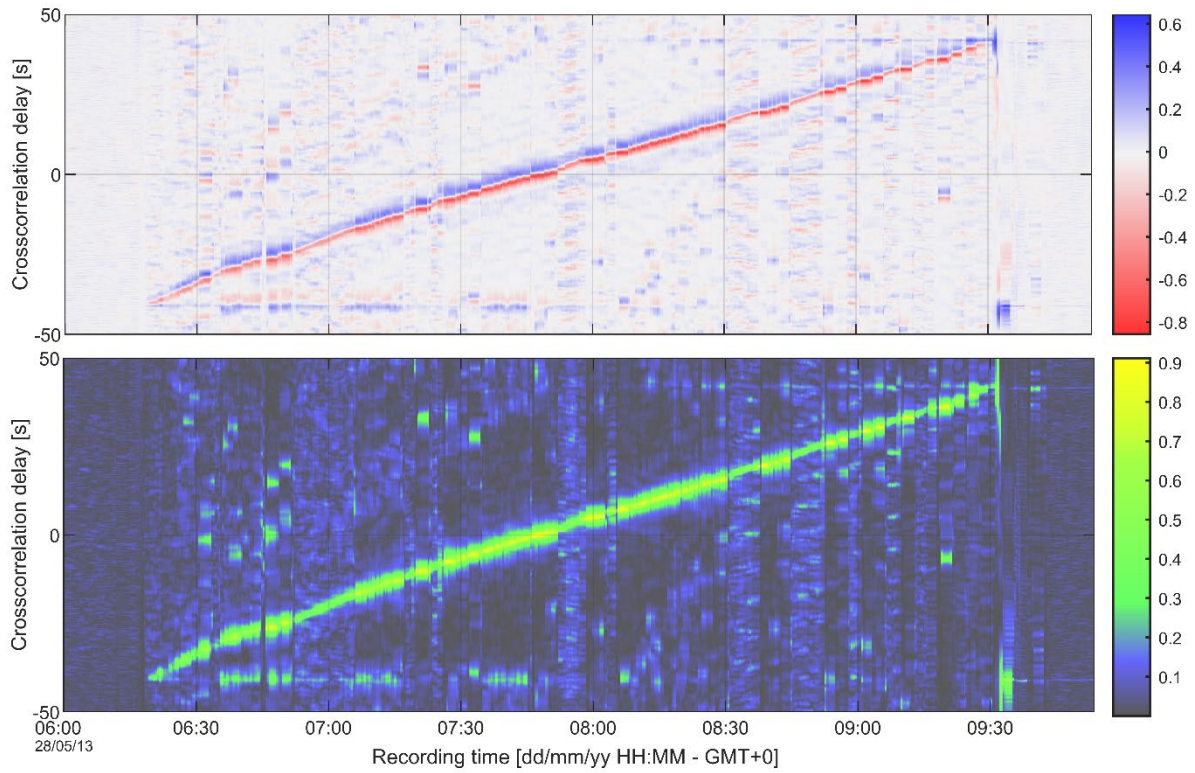


Figure 5. Left: PIG1 tracking on Messina-Favazzina natural gas pipeline (May 7th, 2013); the white arrow indicates a change of PIG1 velocity. Right: PIG2 tracking on Messina-Favazzina natural gas pipeline (May 9, 2013). The white arrows indicate a stop of the PIG.



*Figure 6. PIG3 tracking on Messina-Favazzina natural gas pipeline (May 28, 2013). Normalized crosscorrelation waterfall of pressure signal at Messina and Favazzina: raw crosscorrelation (top) and positive envelope of crosscorrelation (bottom). The PIG “time position” is in the negative reddish peak of the top figure.*

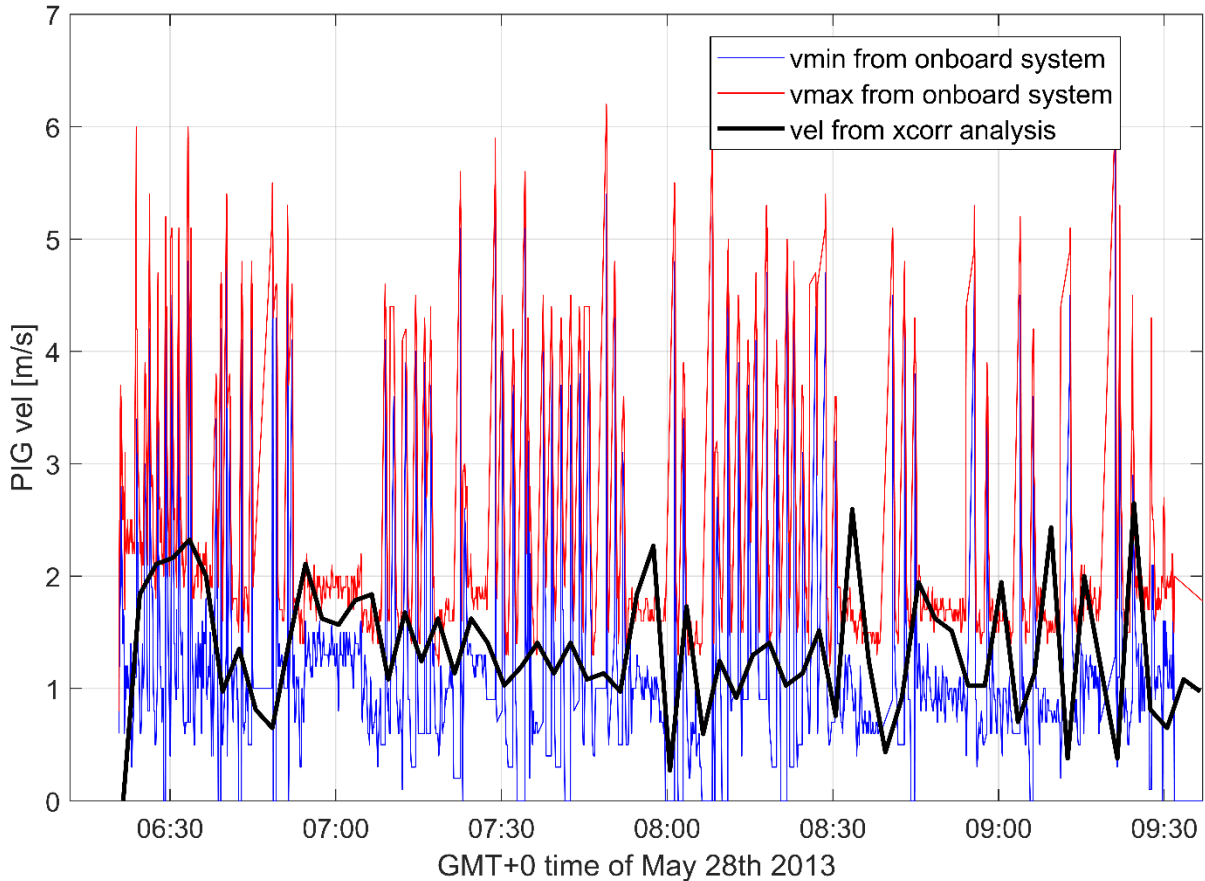


Figure 7. Comparison of velocity tracking procedures (PIG3 operation).

## 2.2. PIG tracking method 2: welding hits counting

A second tracking procedure can be implemented by identifying and counting the sound produced by the PIG at the welding dents. In this case only one station is necessary, provided the sound emission is detectable. For a known length of the pipe units (usually 12 m), peak counting gives the position of the PIG from the departing station. The length of the pipe unit divided by the time distance between two consecutive peaks gives the instantaneous velocity of the gauge.

In order to reduce and unbiased the effects of errors in the peak identification (missed and/or false detections), we have found that it is better to obtain first an average velocity over 4-5 consecutive peaks, and then to compute the PIG position by multiplying the (time varying) average velocity for the time distance between adjacent peaks.

Short Time Average over Long Time Average (STA-LTA) of the pressure signal is an efficient tool to highlight the sound peaks (Trnkoczy, 2012), as they are short wavelets (~1s) with respect to the repetition rate (4-15s). A threshold in the output signal, to be chosen interactively by the user, enables the identification of the peaks.

Referring to Figure 4,  $s(t)$  is the vibroacoustic signal recorded by a generic station along the pipeline.

The STA-LTA signal  $x_{STA-LTA}(t)$  is computed here as

$$x_{STA-LTA}(t) = \frac{T_L \int_{-T_S/2}^{T_S/2} |s(t)| dt}{T_S \int_{-T_L/2}^{T_L/2} |s(t)| dt}, \quad (6)$$

where  $T_S$  and  $T_L$  (with  $T_S < T_L$ ) are the durations of the short time and long time windows, respectively.

Figure 8 shows the pressure signal measured at the departing (Messina) and arriving (Palmi) station during PIG4 operation (Table 1). In this particular case the signal at the departing station is noisy, and the PIG tracking with the crosscorrelation analysis is less effective (Figure 8, A and B). On the other hand, pressure signal at the arriving station displays clear peaks for the PIG crossing the weldings, starting at the PIG launch time (Figure 8.E).

We apply a Short Time Average over Long Time Average (STA-LTA) procedure in order to highlight and identify the peaks of the pressure signal (Figure 9), and we calculate the PIG velocity by measuring the time distance between adjacent peaks, related to the displacement of one 12 m pipe unit. Figure 10 is the comparison of the gauge velocity from on-board measurements (“vmin” and “vmax”) and from the hit count procedure.

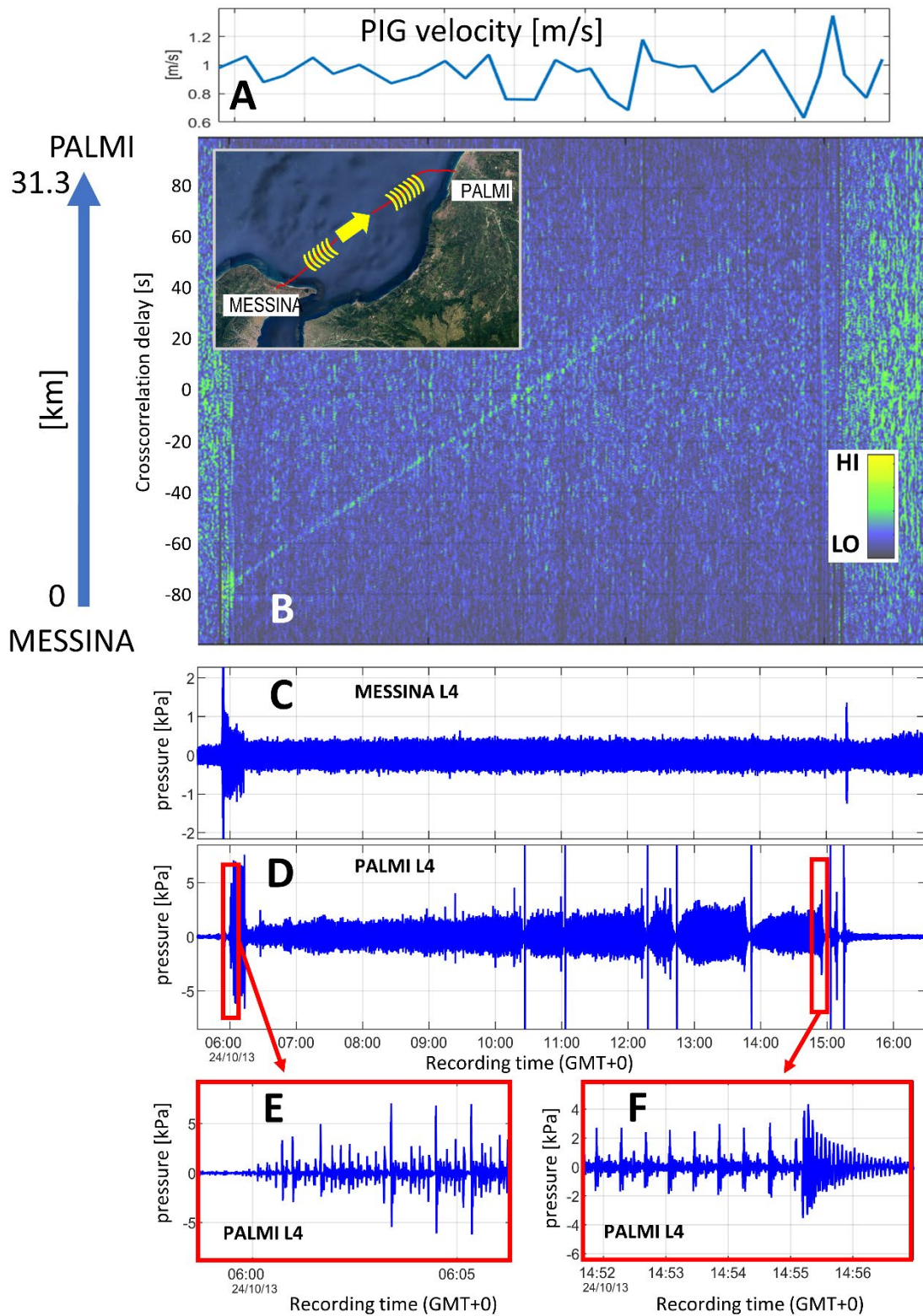


Figure 8. PIG4 tracking on Messina-Palmi LINE4 natural gas pipeline (October 24th, 2013). PIG velocity from crosscorrelation processing (A). Crosscorrelation waterfall (B). Pressure transients at Messina (C) and at Palmi (D). Zoom of pressure transients at Palmi station (E and F), welding hits are visible from PIG departure (E).

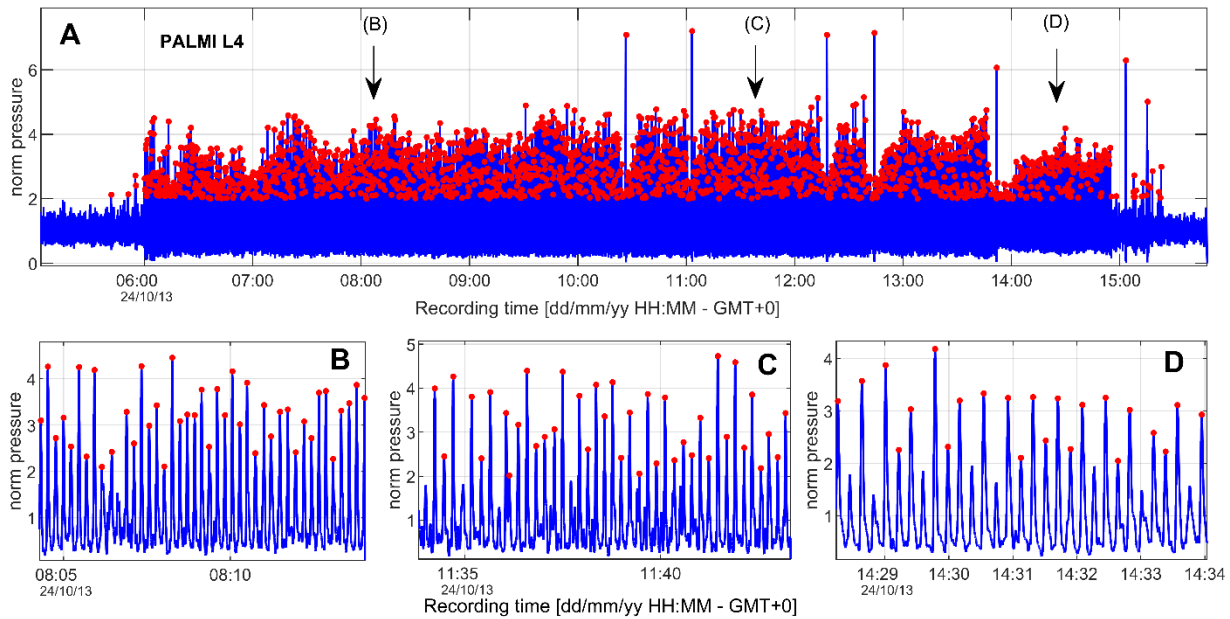


Figure 9. Top (A): PIG4 acoustic signal processing (STA-LTA) and peak detection (red markers) for the whole PIG campaign. Bottom: zooms of some minutes of the signal in A, at the position of the arrows (B, C and D).

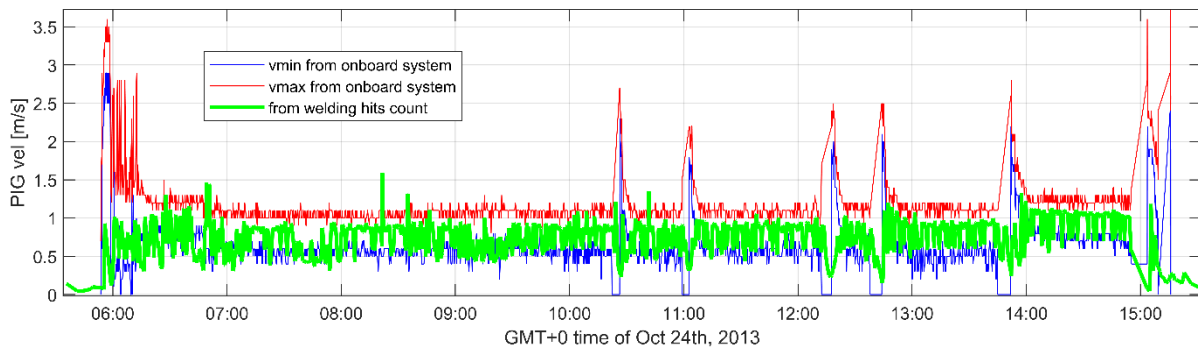


Figure 10. Comparison of velocity tracking procedures (PIG4 operation).

### 3. OFFSHORE SCENARIO: TRANSMED NATURAL GAS PIPELINE

This section presents an original procedure of remote PIG localization, which is applicable when the device is pushed at low differential pressure, and so its movement is a sequence of start and stop intervals, where the stop one is several minutes long. The procedure is illustrated on a real scenario. On July 2009, in the framework of a research project, a vibroacoustic monitoring system has been installed on a natural gas transportation line of the TRANSMED network, at Mazara del Vallo terminal (Sicily). The pipe has an internal diameter of 20" and a length of 155 km between Cape Bon pumping station (Tunisia) to Mazara del Vallo terminal (Sicily). During the inspection campaign, different PIGs have been used for integrity assessment.

#### 3.1. PIG tracking method 3: pipeline resonance

We analyse here the vibroacoustic signal produced by a PIG sent on August 25<sup>th</sup>, 2009, from Cap Bon, and arrived at Mazara del Vallo at 17.20 GMT+0, August 26<sup>th</sup>, 2009. The pipeline was filled with

air at around 8 bars. Differential pressure at the PIG sides was around 2 bar. The PIG movement is discontinuous, with stop intervals of some minutes and sudden motion of tens of seconds (Hendrix et al., 2018).

Figure 11.A shows the dynamic pressure signals within the pipe at the arrival terminal (Mazara del Vallo). The arrows highlight some amplitude peaks in the time plot (pressure >1kPa), as well as in the spectrogram (B): they correspond to gauge movement, detectable some hours before its arrival in Sicily. Every PIG stop creates a pressure wave that propagates in the pipeline. The rest duration permits the generation of a stationary wave within the free cylindrical pipeline section, closed at the PIG position by the gauge itself, and open at the onshore receiving terminal, where an open-air vent was installed.

A tube of air resonates at multiple frequencies of a fundamental one (first harmonic), which in turn is a function of the pipe length and of the end conditions. A closed end is a displacement node in the standing wave, an open end behaves like a displacement antinode. Displacement nodes are pressure antinodes and viceversa (Mechel, 2004). Figure 11 (left) explains this effect and computes the stationary frequencies, that result to be the odd multiples of the fundamental harmonic

$$f_1 = \frac{v_{sound}}{4L}, \tag{7}$$

with  $L$  the free pipeline length and  $v_{sound}$  the sound speed in air.

The principal frequency is detectable together with some higher harmonics in Figure 11.B. Using an estimated sound speed of 340 m/s, it is possible to obtain the distance of the PIG from the arrival terminal (bottom of Figure 11.B).

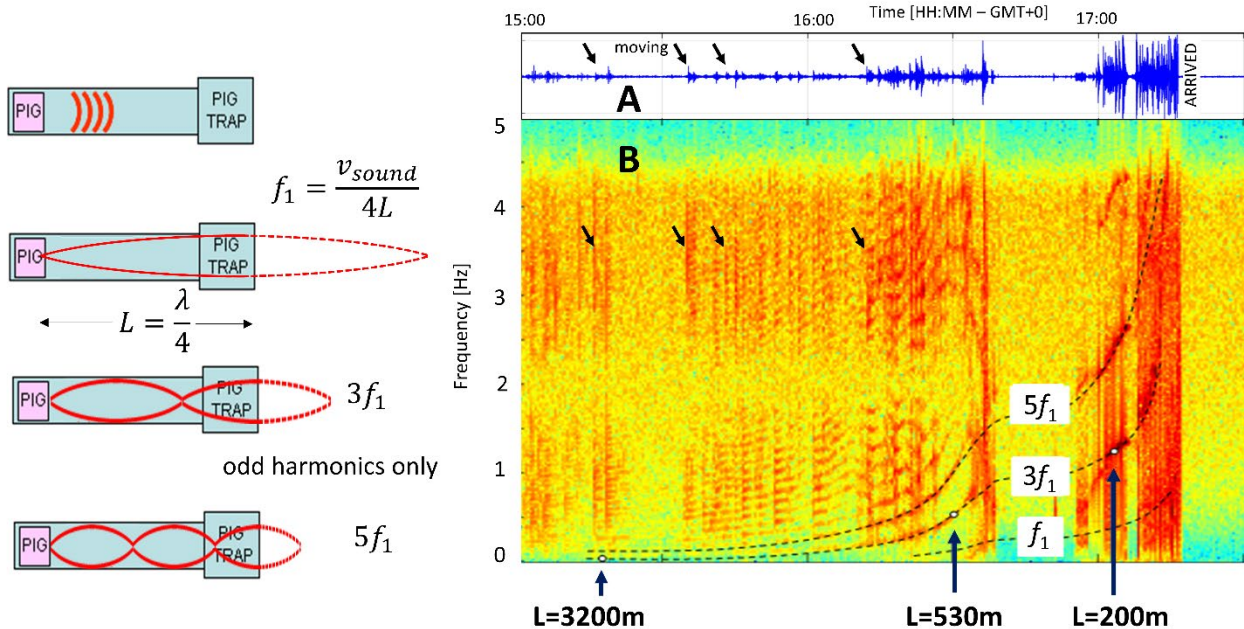


Figure 11. Right: pressure signal (A) and spectrogram (B) at the receiving terminal of a PIG (Mazara del Vallo, August 26<sup>th</sup>, 2009, GMT+0 time). Arrows indicate some events of PIG movement. Time to distance conversion with an estimated sound velocity of 340 m/s.  $L$  is the distance of the PIG to the arrival. Left: scheme of PIG-induced stationary waves.

#### 4. ONSHORE SCENARIO: CRUDE OIL TRANSPORTATION PIPELINE

For sake of completeness we show here an example of PIG tracking for a liquid fluid (crude oil) transportation pipeline. The satellite map is shown in Figure 12.D. The vibroacoustic data has been collected from 2010 to 2015 at different stations (VM) along the oil pipeline, managed by Eni Downstream in North of Italy. Pipeline length is around 100 km, pipe internal diameter is 16", and crude oil pressure varies between 60-70 bars at the pumping station VM213, down to 3-4 bars at the receiving terminal VM301.

We use the pressure transients recorded at the departing terminal (VM213) and at station VM35, 59.7 km apart, to monitor a pigging operation run on August 21<sup>st</sup>, 2013.

Figure 12.C is the result of the crosscorrelation procedure: the PIG can be tracked in position and velocity for the whole run. It is interesting to notice that the crossing of valves produces a different wavelet with respect to the crossing of the welding dents, the valves appearing like an amplitude anomaly in the crosscorrelation peak. In Figure 12.C it is possible to distinguish the case of nearby double valves (before and after rivers and/or railways crossings, tagged with the letter "a"), from the amplitude anomaly at single valves (e.g. non return valves, tagged with the letter "b").

The peak count procedure can be applied up to 3-4 hours after the PIG launch, as the peaks become unclear also from the recordings of the closest stations (Figure 13). Nevertheless, we have computed a density plot using the automatically tracked events (Figure 12.A), which is still accurate up to around 20 km of PIG displacement.

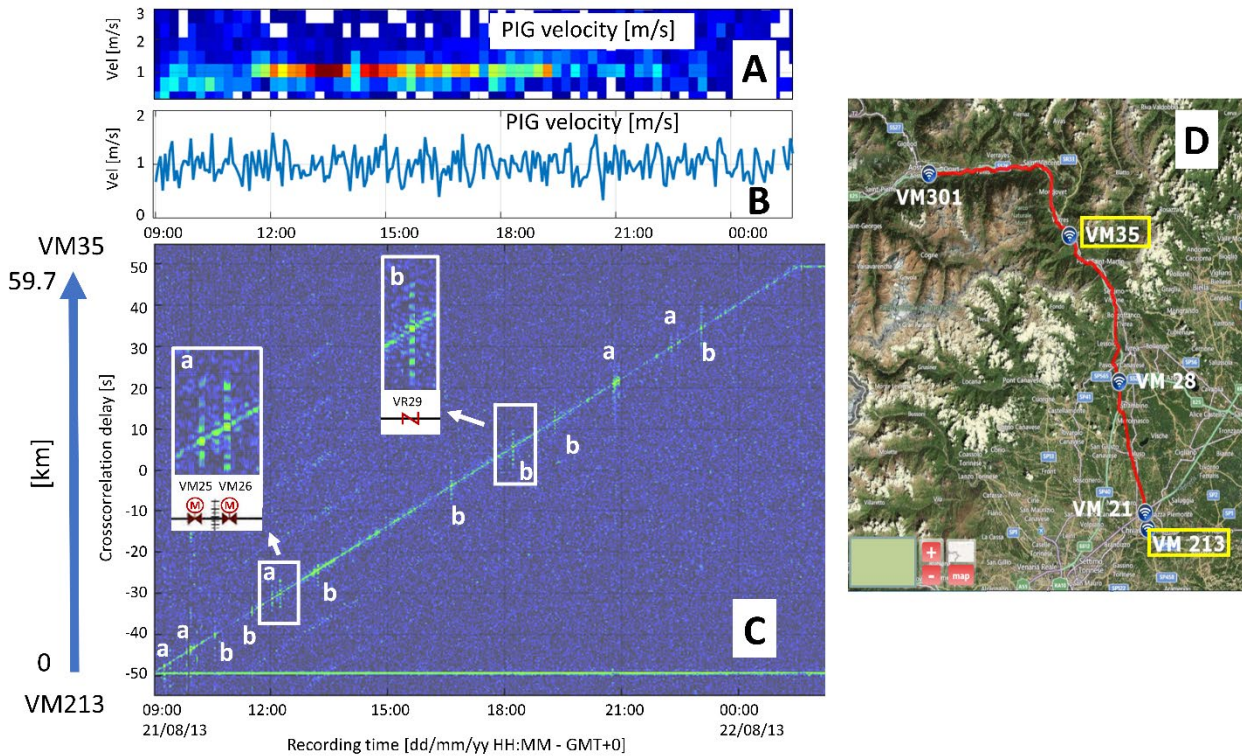


Figure 12. Satellite map of the crude oil pipeline route (D): vibroacoustic monitoring stations are highlighted. PIG tracking with the crosscorrelation procedure of the signals at station VM213 and VM35 (C). The crosscorrelation peak shows also the crossing of single valves (b) and of nearby double valves (a). PIG velocity from the crosscorrelation analysis (B) and from the hit count procedure (A).

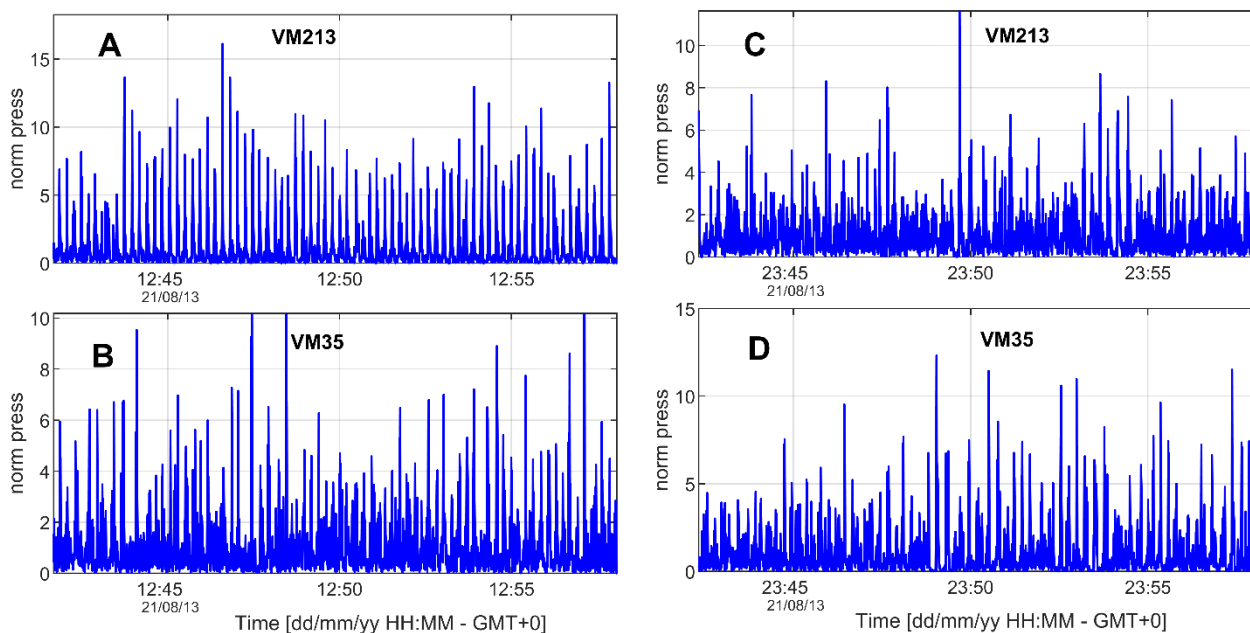


Figure 13. STA-LTA processing of the pressure signal for the hit count analysis. Panels A and B: the PIG is at around 15 km from the departure (VM213), but the peaks are visible also at the arriving station (VM35), around 45 km apart. Panels C and D: the PIG is at 15 km to the arrival (VM35), the peaks are unclear.

## 5. ACOUSTIC MODEL FOR TRAVELLING PIGS

This section reports a simplified model of sound propagation within a pipeline that is used to estimate the maximum operational distance for a PIG tracking procedure. A pipeline behaves like a waveguide for pressure signals traveling within the fluid. The pressure transients are generated by flow/pumps regime variations, opening of holes (leaks), valve movements, and by hits on the pipe shield, as the ones produced by the sealing cups of a travelling PIG when crossing a welding dent. Acoustic wave propagation in fluid filled pipes is mainly governed by the dispersion curves (dependence of the wave velocity on frequency, for each mode), and by the attenuation curves (decay of the signal amplitude with propagation distance). Dispersion and attenuation on their side depend on the fluid and pipe parameters (Elvira-Segura, 2000), namely on:

- fluid bulk viscosity and thermal conduction;
- fluid viscous and thermal interaction with the pipe wall;
- fluid relaxation;
- pipe visco-elasticity;
- pipe external load.

Here we use the “wide-tube approximation” modeling, which comes from the results of Kirchhoff (1868). Absorption is related only to interaction with the pipe wall, which takes place in a narrow boundary layer, with respect to the pipe radius (Blackstock, 2000). The absorption coefficient  $\alpha$  and the phase velocity  $v_{sound}$  are functions of the angular frequency  $\omega$ , the pipe radius  $b$ , and the fluid physical properties (density  $\rho_f$ , speed of sound in the free medium  $v_0$ , dynamic viscosity  $\eta$ , specific heats ratio  $\gamma$  and Prandtl number  $Pr$ ):

$$\alpha = \frac{1}{b} \sqrt{\frac{\omega \eta}{2 \rho_f v_0^2}} \left( 1 + \frac{\gamma - 1}{\sqrt{Pr}} \right) \quad (8)$$

$$v_{sound} = \frac{v_0}{1 + \alpha v_0 / \omega} \quad (9)$$

The absorption coefficient is proportional to the square root of the frequency and inversely proportional to the pipe radius.

The model is applicable when the pipe rigidity is much higher than the fluid rigidity. In order to take into account pipe elasticity, we replace the free medium fluid sound speed  $v_0$  with the celerity  $\hat{v}_0$  of water-hammer pressure waves in pipelines, which depends on the ratios between the pipe radius and the wall thickness  $b/w_t$ , and between the fluid and pipe compressibility  $B_f/E$  (Blackstock, 2000),

$$\hat{v}_0 = \frac{\sqrt{B_f / \rho_f}}{\sqrt{1 + (B_f / E)(2b / w_t) \varepsilon}}, \quad (10)$$

where  $\varepsilon$  is a dimensionless factor, equal to 1.0 when the pipe wall is thin (i.e., when  $2b/w_t > 25$ ). Notice that  $\hat{v}_0$  is always less than  $v_0$ , so the elasticity of the pipe walls has the effect of reducing the wave speed.

We have found that at low frequency (<20 Hz) this model can be applied both to gases and liquids (Giunta et al., 2015), as the principal reason of attenuation is the viscous effect (plus the thermal effect in gases). The radiation of energy in the medium surrounding the pipe becomes important, for liquids, at medium-high frequencies (up to 100 Hz), while remains negligible for gas filled pipes.

### 5.1. Estimation of PIG detection distance in pipelines

We estimate the maximum PIG detection distance by evaluating the acoustic decay curve of the “welding crossing” sound. We consider the PIG operation along the Messina-Palmi natural gas line (PIG4, Table 1). Figure 8.D is the pressure signal at Palmi: hit sounds are well distinguishable for the whole operation. Figure 14.A plots the energy (dB) of the peaks versus travelled distance, fitted with a linear decay curve (exponential decay for a linear energy scale, as predicted from theory). The estimated decay is around 0.2-0.3 dB/km, in agreement with the wide tube formula in the same frequency range, i.e. [1-10Hz] for the natural gas (Figure 14.C). Figure 14.A shows also that the noise level is around -20dB.

The estimated maximum detection, when using a single side detection, is around 80-100km, when hit peaks reach the noise level. If the signal is visible from both sides, this distance could be doubled. Please remember scenario conditions are:

- ILI – MFL PIG;
- 26” ID pipeline;
- around 63 bars at Messina, 60 bars at Palmi.

For the same noise level, maximum detection distance is directly proportional to pipe internal diameter (the higher the diameter, the higher the detection distance) and to the square root of gas pressure.

Figure 14.B shows the energy decay curve computed along the VM213-VM35 oil transportation line, that fits a line with 0.25-0.35 dB/km, in agreement with the theoretical curve in Figure 14.C for a

frequency below 2Hz. Also, for the crude oil the estimated (and observed) maximum PIG detection distance is below 100km.

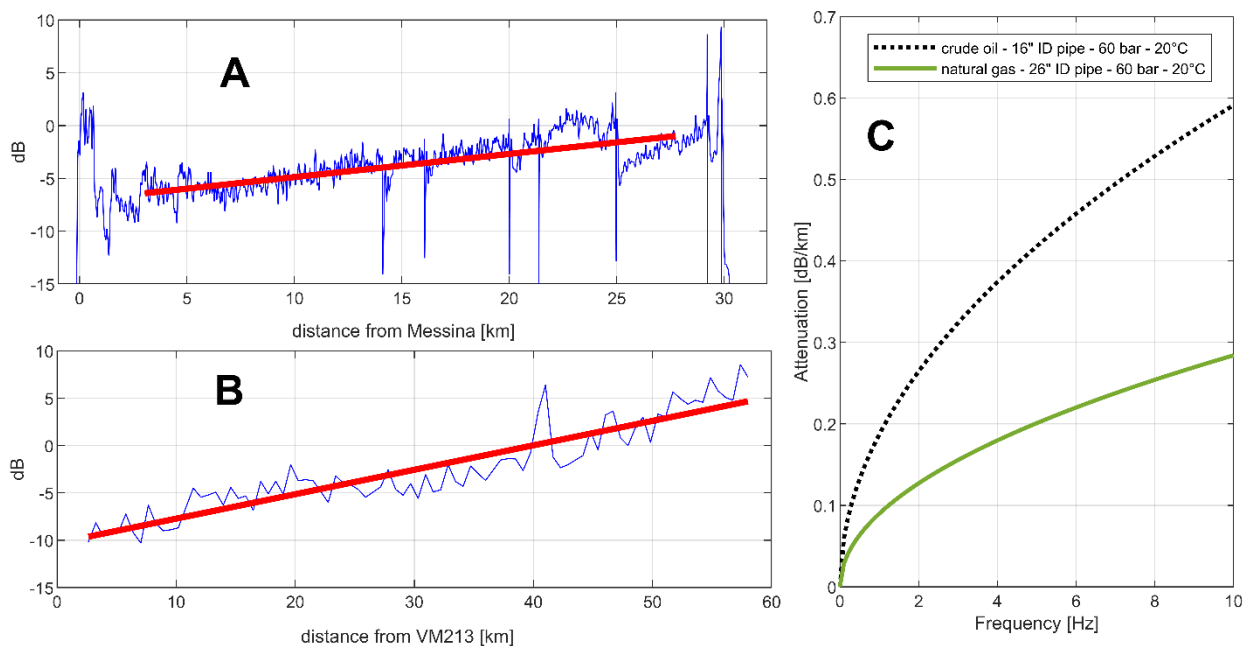


Figure 14. Energy decay curve in the Messina Palmi gas line (A) and in the VM213-VM35 crude oil line (B). Theoretical attenuation for the scenarios oil & gas in the figure (C).

## 6. CONCLUSIONS

Pipeline inspection with internal gauges (PIGs) is an important option for monitoring the asset integrity. Moreover, the real time tracking of the inspection tool increases the safety and the efficacy of the operation. The current technology for locating a travelling PIG makes use of active systems mounted on the PIG or of sensors deployed along the line that are triggered by the nearby passage of the device, so increasing the complexity and the cost of the campaign.

On the other hand, travelling PIGs are themselves active sources: vibroacoustic transients are produced when they slide against the inner pipe wall and when they cross the welding dents. These transients, of the order of 1-5 kPa (10-50 mbar), are guided by the fluid line for long distances from the originating location. This paper has presented three different procedures that exploit the PIG noise to remotely track its position and velocity during the inspection. The procedures have been successfully validated with experimental campaigns. The input data are the real time synchronized recordings of the pressure transients that propagate in the fluid, collected on a discrete set of points along the line with a relative distance of tens of kilometres, made available for multichannel processing on a central unit. The system can be assembled with off-the shelf components, using GPS time synchronization and data transmission through the mobile network. No special instrumentation has to be mounted on the travelling gauge. The technological platform then looks safer and competitive with respect to the actual solutions, or at least complementary when the distances between the recording stations permit to “hear” the sound produced by the PIG. Offshore scenarios are a very special case, as the distance between accessible platforms and/or onshore terminals is usually below the estimated 100km of detection capability for pipelines with an internal diameter greater than 10”, so permitting to operate a PIG tracking along the whole pipeline without complex and expensive submarine equipment.

## 7. ACKNOWLEDGMENTS

This research was mainly carried out in the framework of the R&D – DIONISIO project founded by Eni S.p.A. The authors are grateful to SolAres JV team for technical support during the field tests.

## 8. REFERENCES

- Alonso, J. R., 2007, System for locating pigs in single phase and multiphase fluid transport pipelines, Patent WO2009067769A1.
- Barrias, A.; Casas, J.R.; Villalba, S., 2016, A Review of Distributed Optical Fiber Sensors for Civil Engineering Applications, *Sensors*, 16, 748, <https://doi.org/10.3390/s16050748>.
- Bernasconi, G., Del Giudice, S., Giunta, G., Dionigi, F., 2013, Advanced pipeline vibroacoustic monitoring, Proceedings of the ASME 2013 Pressure Vessels & Piping Division Conference, July 14-18, 2013, Paris, France, PVP2013-97281.
- Bernasconi G., S Del Giudice, G Giunta, 2014, Advanced real time and long term monitoring of transportation pipelines, ASME 2014 International Mechanical Engineering Congress and Exposition, <https://doi.org/10.1115/IMECE2014-36872>.
- Blackstock, D. T., 2000, Fundamentals of physical acoustics. John Wiley & Sons, Inc.
- Brayson, A.T., Ignagni, M. B., Touchberry, A. B., Anderson, D. W., Glen, S. J., Gilman, J. M., 1997, Method and apparatus for determining location of characteristics of a pipeline, Patent WO1999032902A2.
- Brown, R. C., McIntyre, J. D., 1986, Pipeline PIG tracking, Patent EP0122704A2.
- Carter G.C., 1985, Time Delay Estimation. In: Urban H.G. (eds) Adaptive Methods in Underwater Acoustics. NATO ASI Series (Series C: Mathematical and Physical Sciences), vol 151. Springer, Dordrecht, [https://doi.org/10.1007/978-94-009-5361-1\\_15](https://doi.org/10.1007/978-94-009-5361-1_15).
- Chen, J., Luo, X., Zhang, H., He, L., Chen, J., Shi, K., 2018, Experimental study on movement characteristics of bypass pig, *Journal of Natural Gas Science and Engineering*, 59, 212-223, <https://doi.org/10.1016/j.jngse.2018.08.023>.
- Chowdhury, M. S., Abdel-Hafez, M. F., 2016, Pipeline Inspection Gauge Position Estimation Using Inertial Measurement Unit, Odometer, and a Set of Reference Stations, *ASME J. Risk Uncertainty Part B*. June 2016; 2: 021001. <https://doi.org/10.1115/1.4030945>
- Davoudi, M., Heidari, Y., Mansoori. S.A.A., 2014, Field experience and evaluation of the South Pars sea line pigging, based on dynamic simulations, *Journal of Natural Gas Science and Engineering*, 18, 210-218, <https://doi.org/10.1016/j.jngse.2014.02.013>.
- Elvira-Segura, L., 2000, Acoustic wave dispersion in a cylindrical elastic tube filled with a viscous liquid, *Ultrasonics* 37, 537-547, [https://doi.org/10.1016/S0041-624X\(99\)00107-9](https://doi.org/10.1016/S0041-624X(99)00107-9).
- Esmaeilzadeh, F., Mowla, D., Asemani, M., 2009, Mathematical modeling and simulation of pigging operation in gas and liquid pipelines, *Journal of Petroleum Science and Engineering*, 69, Pages 100-106, <https://doi.org/10.1016/j.petrol.2009.08.006>.
- Feldman, M., 2009, Hilbert Transform, Envelope, Instantaneous Phase, and Frequency, *Signal Processing*, Wiley, <https://doi.org/10.1002/9780470061626.shm046>
- Giunta, G., Bernasconi, G., Del Giudice, S., 2015, Pipeline Monitoring with Vibroacoustic Sensing, *Materials Evaluation*, Vol.73 (7), pp. 979-986.
- Giunta, G., Bernasconi, G., 2017a, Method and system for the remote detection of the position of a pig device inside a pressurized pipeline, Patent EP2935969B1 (2017) and US9897243B2 (2018).

- Giunta, G., Bernasconi, G., Del Giudice, S. 2017b, Method and system for the continuous remote tracking of a pig device and detection of anomalies inside a pressurized pipeline, Patent EP294485700B1 (2017) and US10132823B2 (2018).
- Giunta, G., Bernasconi, G., 2017c, Method and system for continuous remote monitoring of the integrity of pressurized pipelines and properties of the fluids transported, Patent EP2936106B1 (2017) and US10401254B2 (2019).
- Gudmundsson, J.S., 2017, Flow Assurance Solids in Oil and Gas Production, CRC Press.
- Hendrix, M.H.W., Graafland, C.M., van Ostayen, R.A.J., 2018, Frictional forces for disc-type pigging of pipelines, *Journal of Petroleum Science and Engineering*, 171, 905-918, <https://doi.org/10.1016/j.petrol.2018.07.076>.
- Hendrix, M.H.W., Ijseldijk, H.P., Breugem, W.P., Henkes, R.A.W.M., 2018, Experiments and modeling of by-pass pigging under low-pressure conditions, *Journal of Process Control*, 71, 1-13, <https://doi.org/10.1016/j.jprocont.2018.08.010>.
- Hartog, A.H., 2017, An Introduction to Distributed Optical Fibre Sensors; CRC Press: Boca Raton, FL, USA, <https://doi.org/10.1201/9781315119014>.
- Hiltscher, G., Muhlthaler, W., Smits, J., 2003, Industrial Pigging Technology- Fundamentals, Components, Applications, Wiley VCH, Weinheim, <https://doi.org/10.1002/352760913X>.
- Kirchhoff, G., 1868, Ueber den Einfluss der Wirmeleitung in einem Gase auf die Schallbewegung, *Poggendorfer Annalen*, 134, 177-193, <https://doi.org/10.1002/andp.18682100602>.
- Liang Z., He, H., Cai W., 2017, Speed simulation of bypass hole PIG with a brake unit in liquid pipe, *Journal of Natural Gas Science and Engineering*, 42, 40-47, <https://doi.org/10.1016/j.jngse.2017.03.011>
- McAllister, E. W., 1998, Pipeline Rules of Thumb Handbook: A Manual of Quick, Accurate Solutions to Everyday Pipe Line Engineering Problems. Gulf Publishing Company, Houston.
- Mechel, F.P., 2004, Duct Acoustics, Mechel F.P. (eds) *Formulas of Acoustics*. Springer, Berlin, Heidelberg, <https://doi.org/10.1007/978-3-662-07296-7>.
- Nguyen, T. T., Sang B. K., Hui R. Y. & Yong W. R., 2001, Modeling and simulation for PIG flow control in natural gas pipeline, *KSME International Journal*, 15, 1165–1173, <https://doi.org/10.1007/BF03185096>.
- Patricio, R.A.C., Baptista, R.M., de Freitas Rachid, F.B., Bodstein, G.C.R., 2020, Numerical simulation of pig motion in gas and liquid pipelines using the Flux-Corrected Transport method, *Journal of Petroleum Science and Engineering*, Volume 189, <https://doi.org/10.1016/j.petrol.2020.106970>.
- Tanimola, F.; Hill, D., 2009, Distributed fibre optic sensors for pipeline protection, *J. Nat. Gas Sci. Eng.*, 1, 134–143, <https://doi.org/10.1016/j.jngse.2009.08.002>.
- Tiratsoo, J.N.H., 1999, Pipeline Pigging Technology, Gulf Publishing Company, Houston.
- Tolmasquim, S.T., Nieckele, A.O., 2008, Design and control of pig operations through pipelines, *Journal of Petroleum Science and Engineering*, 62 (3), 102 - 110, <https://doi.org/10.1016/j.petrol.2008.07.002>.
- Trnkoczy, A., 2012, Understanding and parameter setting of STA/LTA trigger algorithm, Bormann, P. (Ed.), *New Manual of Seismological Observatory Practice 2 (NMSOP-2)*, Potsdam, Deutsches GeoForschungsZentrum GFZ, 1-20
- Wang, H. J., Zhang, S. M., Zhang, P., Shi, L. Y., 2010, The Pig Tracking System Based on AVR Microcontroller and GPS/GSM. *Advanced Materials Research*, 139–141, 2195–2198. <https://doi.org/10.4028/www.scientific.net/amr.139-141.2195>

Zhang, H., Zhang, S., Liu, S., Wang, Y, Lin, L., 2015, Measurement and analysis of friction and dynamic characteristics of PIG's sealing disc passing through girth weld in oil and gas pipeline, *Measurement*, 64, 112-122, <https://doi.org/10.1016/j.measurement.2014.12.046>.

## LIST OF FIGURE CAPTIONS

*Figure 1. Messina channel subsea natural gas transportation pipelines. In red the tracks of LINE 1 (15.9 km length, internal diameter ID=20") and LINE 4 (31.3 km length, internal diameter ID=26").*

*Figure 2. Dynamic pressure standard deviation computed every 10 s for PIG1 at Messina terminal (L1) and at Favazzina terminal (L1) (GMT+0 time).*

*Figure 3. Dynamic pressure at Messina terminal for PIG1 in LINE1: zoom on 8 minutes in (A), zoom on 20 s in (B). Time axis in GMT+0.*

*Figure 4. Moving PIG and vibroacoustic monitoring system scheme.*

*Figure 5. Left: PIG1 tracking on Messina-Favazzina natural gas pipeline (May 7th, 2013); the white arrow indicates a change of PIG1 velocity. Right: PIG2 tracking on Messina-Favazzina natural gas pipeline (May 9, 2013). The white arrows indicate a stop of the PIG.*

*Figure 6. PIG3 tracking on Messina-Favazzina natural gas pipeline (May 28, 2013). Normalized crosscorrelation waterfall of pressure signal at Messina and Favazzina: raw crosscorrelation (top) and positive envelope of crosscorrelation (bottom). The PIG "time position" is in the negative reddish peak of the top figure.*

*Figure 7. Comparison of velocity tracking procedures (PIG3 operation).*

*Figure 8. PIG4 tracking on Messina-Palmi LINE4 natural gas pipeline (October 24th, 2013). PIG velocity from crosscorrelation processing (A). Crosscorrelation waterfall (B). Pressure transients at Messina (C) and at Palmi (D). Zoom of pressure transients at Palmi station (E and F), welding hits are visible from PIG departure (E).*

Figure 9. Top (A): PIG4 acoustic signal processing (STA-LTA) and peak detection (red markers) for the whole PIG campaign. Bottom: zooms of some minutes of the signal in A, at the position of the arrows (B, C and D)

Figure 10. Comparison of velocity tracking procedures (PIG4 operation).

Figure 11. Right: pressure signal (A) and spectrogram (B) at the receiving terminal of a PIG (Mazara del Vallo, August 26th, 2009, GMT+0 time). Arrows indicate some events of PIG movement. Time to distance conversion with an estimated sound velocity of 340 m/s.  $L$  is the distance of the PIG to the arrival. Left: scheme of PIG-induced stationary waves.

Figure 12. Satellite map of the crude oil pipeline route (D): vibroacoustic monitoring stations are highlighted. PIG tracking with the crosscorrelation procedure of the signals at station VM213 and VM35 (C). The crosscorrelation peak shows also the crossing of single valves (b) and of nearby double valves (a). PIG velocity from the crosscorrelation analysis (B) and from the hit count procedure (A).

Figure 13. STA-LTA processing of the pressure signal for the hit count analysis. Panels A and B: the PIG is at around 15 km from the departure (VM213), but the peaks are visible also at the arriving station (VM35), around 45 km apart. Panels C and D: the PIG is at 15 km to the arrival (VM35), the peaks are unclear.

Figure 14. Energy decay curve in the Messina Palmi gas line (A) and in the VM213-VM35 crude oil line (B). Theoretical attenuation for the scenarios oil & gas in the figure (C).